INTERNATIONAL JOURNAL OF INTEGRATED ENGINEERING
ISSN: 2229-838X e-ISSN: 2600-7916

IJIE

Vol. 16 No. 3 (2024) 133-144
https://publisher.uthm.edu.my/ojs/index.php/ijie

Freestanding Triboelectric-layer Mode Triboelectric Nanogenerator (TENG) via Rotating Circle

Khaled Jalal Mustafa Abd Alnabi[1], L. Lee[1]*

[1] *Faculty of Engineering,*
Multimedia University, Cyberjaya, 63100, MALAYSIA

*Corresponding Author: linilee@mmu.edu.my
DOI: https://doi.org/10.30880/ijie.2024.16.03.013

Article Info

Received: 22 November 2023
Accepted: 1 January 2024
Available online: 12 May 2024

Keywords

Freestanding mode, rotation-disk structure TENG, dielectric-to-dielectric FTENG, R-TENG

Abstract

In a triboelectric nanogenerator (TENG), electricity can be harvested by utilizing an electrostatic charge between two triboelectric materials. This project focused on optimizing the output power of a TENG using mini lathe beads machine for a freestanding triboelectric-layer mode via rotating circle. The TENG is constructed using aluminum electrodes, adhered to teflon (PTFE) on one side while the other rotational side is constructed using different triboelectric layers. The materials used on the rotational side include teflon, silicone rubber, fiberglass, polyvinyl chloride (PVC) and neoprene rubber. These materials are prepared in a circular shape, with a diameter of 50 mm and thickness that varied from0.13 mm to 2 mm depending on the material employed. These materials are shown to be able to produce voltages ranged from 2.5 V to 18 V, while neoprene rubber showed the highest output at 35.02 V. Based on the experimental work, there are several factors that can affect the performance of the TENG, including temperature, size, material durability, rotating speed, and force as well as alignment of the two layers. This project can be implemented to harvest energy from a moving object like the rotation disc structure, such as a moving automobile or a train.

1. Introduction

A variety of mechanical energy sources, including water waves, airflows, and vibrations, can be harvested with TENG in near future. These mechanisms rely on electrostatics and triboelectrification. TENG based on rotational motions (R-TENG), can produce electrical currents within a wide spectrum of frequencies. R-TENGs possess several advantages when compared with other energy harvesting methods such as solar panels and electromagnetic generators. R-TENG charges a range of devices using their high-frequency pulsed current and high-frequency supercapacitors. R-TENG has more versatility in their applications and are more efficient than solar panels. R-TENG can also be more cost-effective as well as environmentally friendly compared to other harvesting technologies because they do not use toxic substances or produce harmful products.

2. Triboelectric Effect

TENG function by utilizing the triboelectric effect, a chemical bond that forms between surfaces of two different materials when they come in contact. To equalize the electrochemical potential of materials, charges move from one to the other during this procedure. During the separation of the materials, certain bonded atoms tend to keep extra electrons, while others tend to give them away. The transferred charges can be electrons or ions/molecules. The triboelectric charge can be produced on the surface as a result of this. In most cases, materials that undergo strong triboelectrification are less conductive or insulate, resulting in the capture and retention of transfer

charges, which build up electrostatic charges. It is believed that this phenomenon has a negative impact on daily life and technology development. However, it is the basis of the TENG, a device that uses this phenomenon to convert mechanical energy into electrical energy [1, 2].

3. Working Mode of TENG

The principle of triboelectrification and electrostatic induction is the same for all types of TENGs. The TENG can be classified into four modes: contact-separation, relative-sliding, single electrode, and freestanding [1]. Each of these modes has its own advantages and disadvantages [2, 5].

3.1 Contact-Separation Mode

Initially, the two friction layers have no electric charge on their surfaces. When friction layers are in contact, normally vertically, the positive and negative surfaces will be equally charged and remain stable on the surface as a result of the electrification effect. Charges on the surface will reach the electrodes on top when the two friction layers start separating. Mechanical energy is eventually converted into electric energy by this charge flow [2].

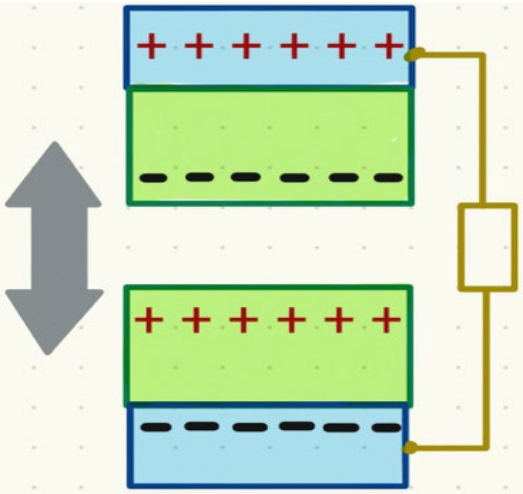

Fig. 1 *A schematic illustration of the contact-separation mode*

3.2 Relative-Sliding Mode

As shown in Fig. 2, the structure starts the same way as vertical contact separation. When two dielectric films are in contact, a relative sliding parallel to the surface also causes triboelectric charges to occur on both surfaces. Therefore, electrons are forced to flow between the electrodes on top and bottom to fully balance the triboelectric charge field due to lateral polarization introduced along the sliding direction. The sliding mode TENG generates

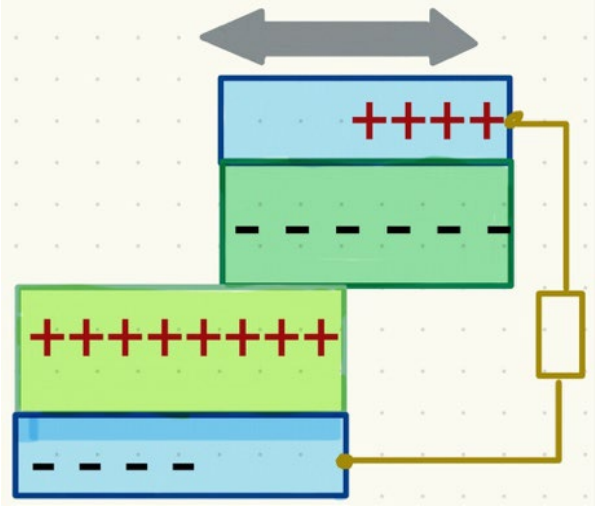

Fig. 2 *Schematic illustration of the linear-sliding mode*

Int. Journal of Integrated Engineering Vol. 16 No. 3 (2024) p. 133-144

an AC output by sliding apart and closing continuously. Planar movements, rotations of cylinders, or rotations of discs may all be used to accomplish this motion [2-4].

3.3 Single-Electrode Mode

The two modes introduced previously had two electrodes interconnected by a load as shown in Fig. 3. In mobile cases, these TENGs can easily be moved. When the TENG object is a mobile object, the connection to the load cannot be made electrically. Taking advantage of such a scenario, a single electrode TENG with a grounded electrode at the bottom was introduced. To maintain potential changes in a finite sized TENG, electron exchanges are required between the bottom electrode and the ground whenever the top object moves from the bottom object. In addition to contact-separation, contact-sliding is also a possibility [2, 4, 6].

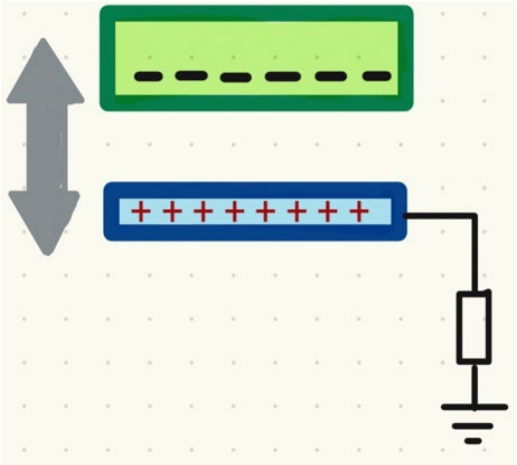

Fig. 3 *Schematic illustration of single-electrode mode*

3.4 Freestanding Mode

In principle, TENG's operation is the same as that of Relative-Sliding Mode, but friction continues throughout the slide. When the outer object moves between the two electrodes, it can utilize the energy of a free-moving triboelectrically charged object to generate an alternative output. As electrostatic induction is significantly more significant than the electrification effect, it is theoretically possible to achieve a maximum energy conversion efficiency of 100% with freestanding mode. In spite of this, the Freestanding design of the movable triboelectric layer makes it difficult to integrate it with other electronic devices and systems [2, 6].

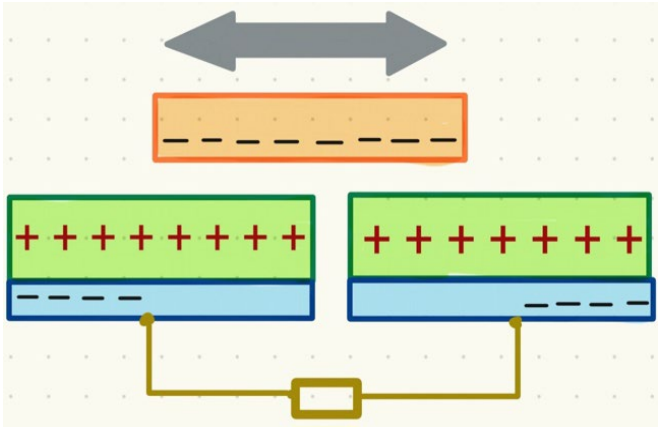

Fig. 4 *Schematic illustration of the freestanding triboelectric-layer mode*

Among various modes, the most efficient technology for harvesting low-frequency sliding energy is the Freestanding mode triboelectric nanogenerator (FTENG). Figure 4 illustrated the freestanding triboelectric- layer mode. Nevertheless, the FTENG encounters limitations such as wastage of half the working area and the presence of contact friction, which significantly curtail its output and durability.

To optimize energy conversion efficiency within this mechanism, one of the triboelectric layers must be connected to a moving object that serves as the mechanical energy source. Unfortunately, in the existing basic modes of TENGs, namely the contact mode [7–10] and the sliding mode [11, 12], each triboelectric layer is linked

to an electrode and a lead wire. This configuration severely restricts the versatility and applicability of TENG for harvesting energy from arbitrary moving objects or walking humans, as the object must be connected to the entire system via an interconnect. Therefore, there is a pressing need to develop a new TENG mode based on an alternative mechanism that can extract energy from the mechanical motion of a freestanding triboelectric layer without requiring an attached electrode.

The fundamental principle behind TENG-based electricity generation lies in the periodic change of the induced potential difference (IPD) between two electrodes, which occurs due to the relative position change of the tribocharged surfaces [8, 11]. This principle can be realized through a novel design and operational mode: a TENG comprising two stationary electrodes and one freestanding triboelectric layer that moves between them under the influence of external mechanical energy. In this mode, the dielectric layer can make direct contact with either one of the metal electrodes or remain in close proximity, facilitating the periodic change of IPD and enabling the flow of charges in the external load. Figure 5 illustrates the three modes present in FTENG: conductor-to-dielectric, conductor-to-dielectric (non-contact sliding mode) and dielectric-to-dielectric.

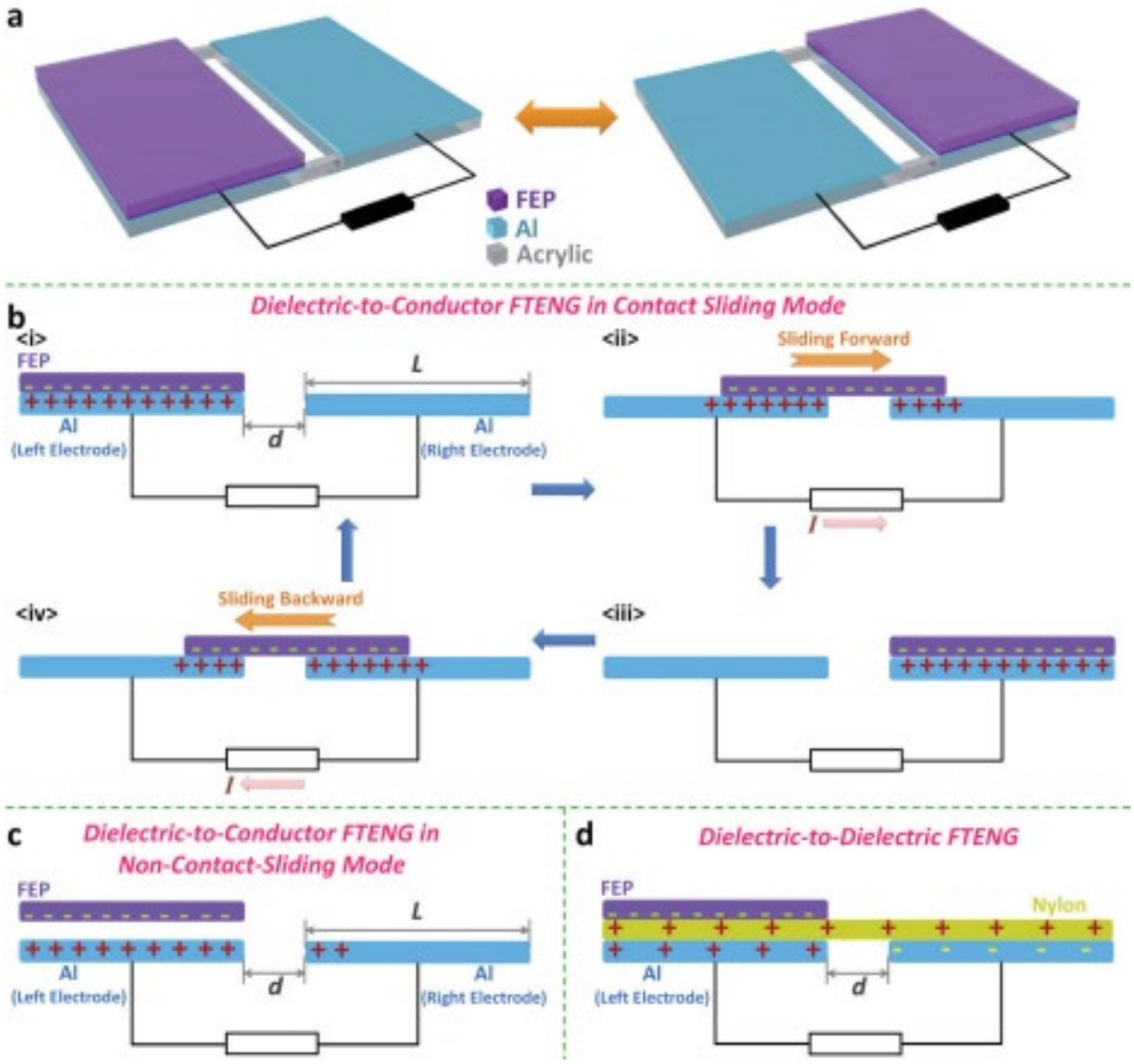

Fig. 5 *This caption provides an overview of the device structure, basic operations, and working principles of the FTENG, including (a) a depiction of the typical structure of a conductor-to-dielectric FTENG; (b) the schematic representation of its working principle in contact sliding mode; (c) schematic diagram illustrating the FTENG in non-contact sliding mode; (d) schematic diagram showcasing the dielectric-to-dielectric FTENG [13]*

Int. Journal of Integrated Engineering Vol. 16 No. 3 (2024) p. 133-144

4. Experimental Setup

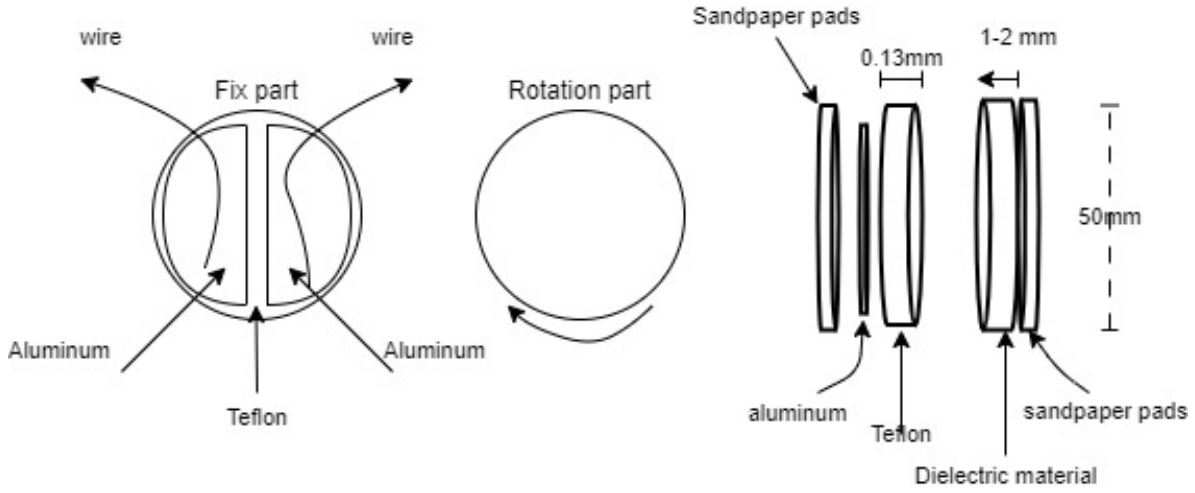

Fig. 6 *Schematic diagram demonstrating the experimental setup used for this research*

In this experiment, a disk rotation structure was utilized as a TENG in a freestanding dielectric-to-dielectric configuration as shown in Fig. 6. This setup featured two metal films, serving dual roles as the counter triboelectric material and the two electrodes. The triboelectric effect was facilitated by a freestanding dielectric layer sandwiched between these two metal films.

Specifically, PTFE was chosen as the material for the freestanding triboelectric layer due to its ability to maximize electrification with other layers, as shown in Fig. 6. To enhance the conductivity of the PTFE layer, an aluminum film was applied to its backside. This film was structured into two half circles that perfectly covered the PTFE circle, which was then securely attached to a sandpaper substrate for support. The substrate not only facilitated easy replacement with other samples but also matched the diameter of the PTFE circle, measuring 5 cm.

For the experiment, the rotating component utilized was the mini lathe beads machine, which incorporated different materials including PTFE, silicone, PVC, fiberglass, and neoprene rubber, as depicted in Fig. 7. The thickness of rotating materials was 1 mm, except for the PVC, which had a thickness of 2 mm. Each experimental setup was observed for a duration of 30 seconds, except when materials experienced frictional breakdown. Notably, for neoprene rubber, the observation period was extended to 57 seconds due to notable changes in values over time.

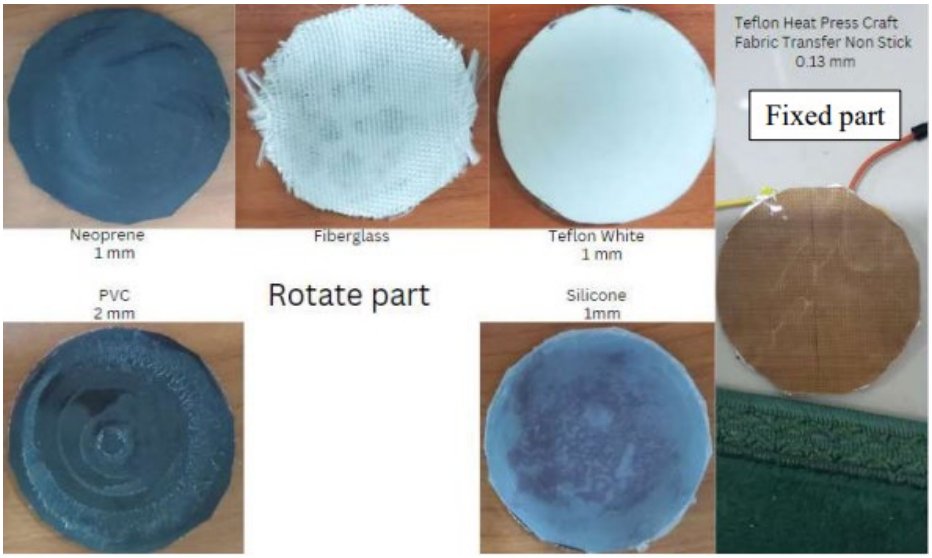

Fig. 7 *Configuration of the materials for the rotating part facing the fixed side PTFE 0.13mm*

The setup was connected to a multimeter for accurate recording of voltage readings from each experiment as demonstrated in Fig. 8. The goals were to identify optimal material combinations for a variety of applications, stabilize the material selection for the freestanding mode, and boost the output of the TENG. The voltage readings were analyzed to ascertain which material combinations offered the highest voltage output and efficiency, with

the findings expected to offer valuable insights into the enhancement of freestanding dielectric-to-dielectric TENG system performance and potential applications.

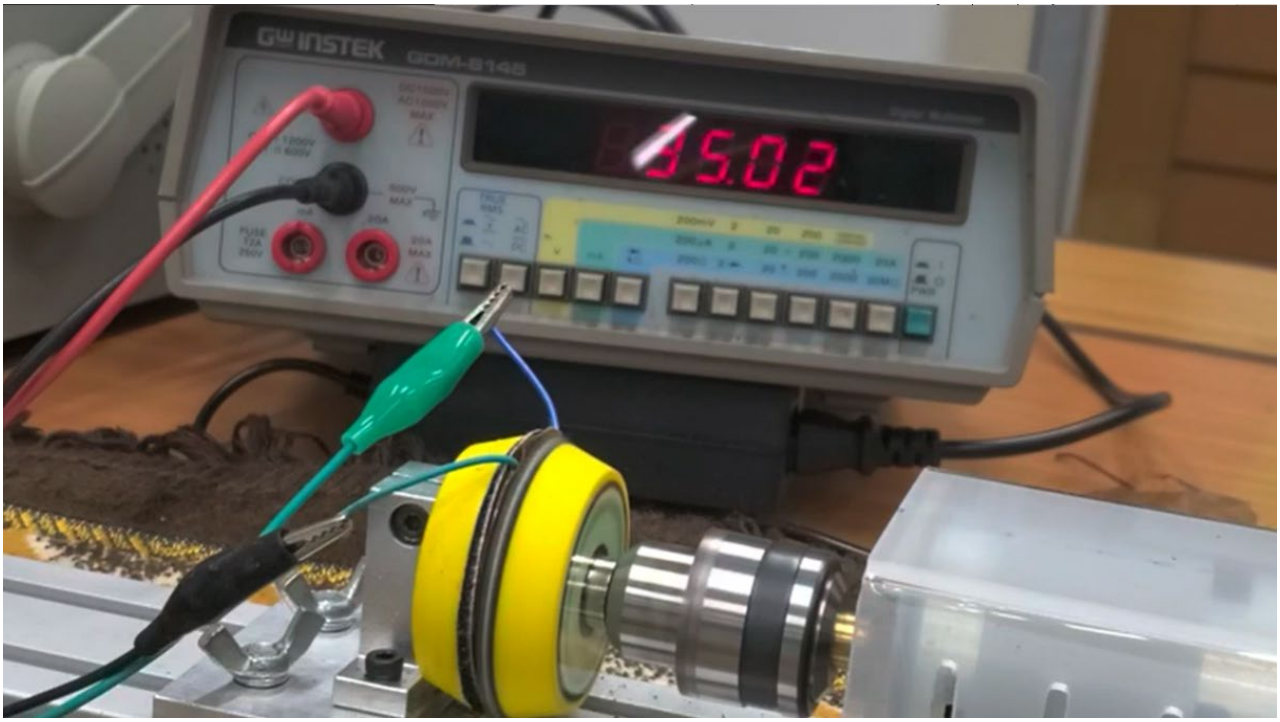

Fig. 8 *Demonstration of how the experiment was conducted and how the multimeter readings were recorded*

To calculate the charge, the capacitance would need to be calculated first using the following equation:

$$C = \varepsilon \frac{A}{D} \quad (1)$$

$$A = \pi r^2 \quad (2)$$

Where C is the capacitance, ε is the air permittivity which is 8.854 x 10-12 F/m, A is the area of the circle which is calculated using Eqn. (2) and D is the distance between the plates. Next, the charge $\boldsymbol{Q}$ was calculated based on Eqn (3), followed by Eqn. (4) for the surface charge density, σ.

$$Q = cv \quad (3)$$

$$\sigma = \frac{Q}{A} \quad (4)$$

where V is the voltage.

5. Result

A freestanding dielectric-to-dielectric TENG was constructed using a series of materials as the triboelectric layer, as demonstrated by the experimental results presented. As a result of the diverse behaviors and responses of these materials, PTFE, silicone, PVC, fiberglass, and neoprene rubber, each with a specified thickness, the TENG provides valuable insight into their suitability for triboelectric applications.

The experiments started with PTFE as the fixed layer. As depicted in Fig. 9, the PTFE maintains an average of around 5 Volts. Given its consistent performance and low wear, it stands as a highly durable material. PTFE is a lightweight material, and its 1mm thickness in this application is advantageous for maintaining a low overall device weight. The output power is relatively clean with no significant surges or dips, and its low wear means that it can contribute to a low- maintenance, long-lasting device. However, its efficiency is limited due to the low voltage output compared to other materials.

Silicone demonstrated the highest voltage output, reaching over 17 volts. While this implies high efficiency, it came at a cost: it damaged the PTFE layer due to friction, suggesting it may have a negative impact on the durability of other system components. Like PTFE, silicone is also lightweight, and the 1mm thickness helps maintain the overall lightness of the device. But, given its potential to harm other materials in the system, it may not provide clean power over extended operation time.

Int. Journal of Integrated Engineering Vol. 16 No. 3 (2024) p. 133-144

PVC initially showed an increased voltage output as illustrated in Fig. 9, suggesting good efficiency. However, the rapid wear and resulting smoke during operation pose significant durability and safety concerns. With 2 to 3mm thickness, it is heavier than PTFE and silicone, which could contribute to a heavier weight. The rapid degradation of PVC under operation means it provides clean power only for a short duration before its performance starts to decline.

The performance of fiberglass was consistent, with a gradual increase in voltage output over time. Its efficiency is, therefore, lower than silicone or PVC but higher than PTFE as show in Fig. 9.

Fiberglass's main disadvantage was the messiness due to the volatility of its fibers, affecting cleanliness and potentially other system components. Depending on the specific type of fiberglass used, it could have a relatively high weight, potentially increasing the total device weight. Its thickness wasn't specified, but it could affect the device's weight and overall durability.

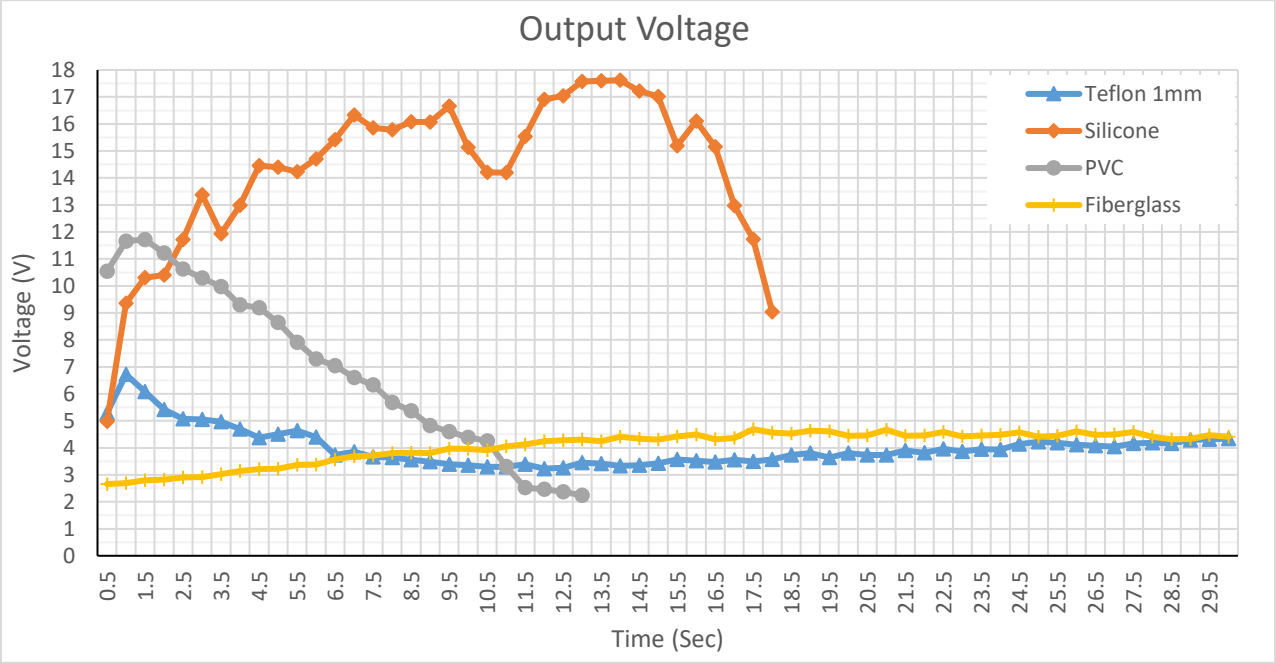

Fig. 9 *Graph showing the output voltage response of TENG with different set when PTFE as fix layer*

Neoprene rubber demonstrated the highest increase in both voltage and temperature over time, showing high efficiency as depicted in Fig. 10. However, the associated high temperature resulted in the substrate material melting over time, raising durability and safety concerns. As a rubber material, neoprene is relatively lightweight, but it tends to be denser than materials like PTFE or silicone. Therefore, it might contribute slightly more to the total device weight. Its power output is not clean over extended periods due to the increased temperature and subsequent melting of the substrate.

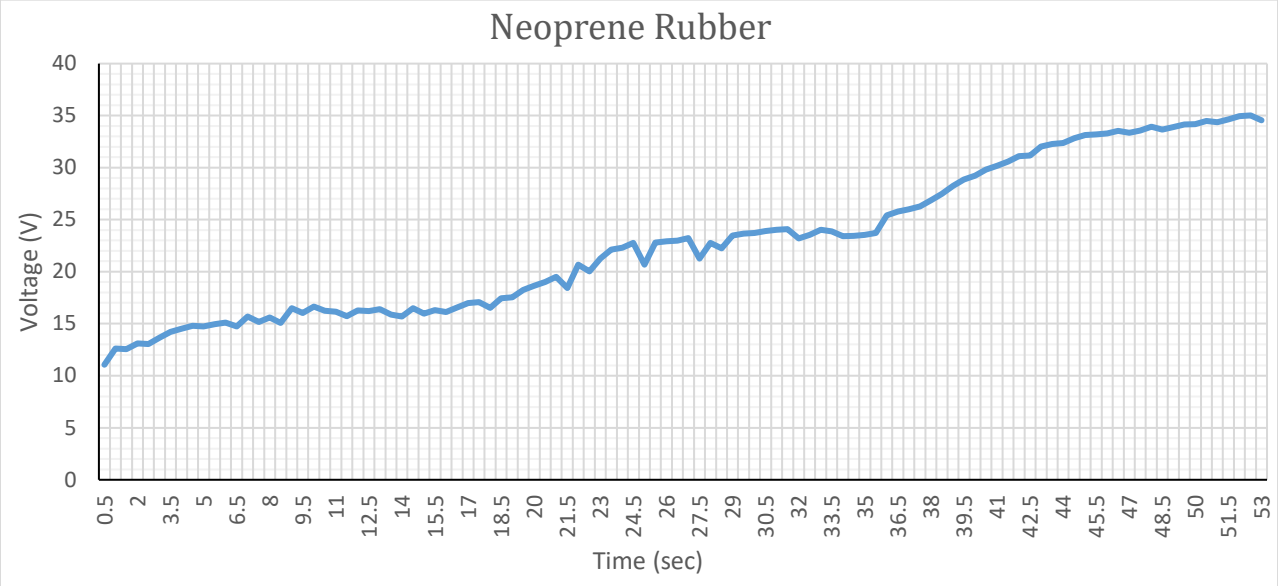

Fig. 10 *Graph showing the voltage response of TENG when neoprene rubber is the triboelectric layer*

The average voltage for each set was then calculated and represented in Table 1.

Table 1 *Average voltage for dielectric-to-dielectric FTENG for each experiments*

Triboelectric Material	Average attained voltage (V)
PTFE	4.400
Silicone	14.313
PVC	6.937
Fiberglass	4.054
Neoprene rubber	22.861

For each experiment, the capacitance value was calculated using equation (6) in order to obtain the capacitance value required for calculating the charges. The charge value was then determined by manually applying equation (7) to each experiment. Finally, equation (8) was used to calculate the surface charge density for each triboelectric layer. For PTFE material, following is an example of the calculations.

$$A = \pi r^2 = \pi \times 0.025 \times 0.025 = 1.9635 \times 10^{-3}\ m^2 \tag{5}$$

$$C = \varepsilon \frac{A}{D} = (8.854 \times 10^{-12}) \frac{(1.9635 \times 10^{-3} m)}{0.01} = 1.7446 \times 10^{-11} F \tag{6}$$

$$Q = C \times V_{avg} = (1.7446 \times 10^{-11}) \times 4.3999 = 7.6761 \times 10^{-11} C \tag{7}$$

$$\sigma = \frac{Q}{A} = \frac{7.6761 \times 10^{-11}}{(1.9635 \times 10^{-3} m)} = 3.9094 \times 10^{-8} \frac{c}{m^2} \tag{8}$$

In Table 2, we can see that neoprene rubber has the highest surface charge density when facing PTFE 0.013mm on the fixed side.

Int. Journal of Integrated Engineering Vol. 16 No. 3 (2024) p. 133-144

Table 1 *Calculated charge for each set of dielectric-to-dielectric FTENG*

Triboelectric Layer	Calculated Capacitance (F)	Calculated Charge (C)	Surface charge density ($C.m^{-2}$)
PTFE		7.6761×10^{-11}	3.9094×10^{-8}
Silicone		2.497×10^{-10}	1.272×10^{-10}
PVC	1.7446×10^{-11}	1.210×10^{-10}	6.162×10^{-11}
Fiberglass		7.073×10^{-11}	3.602×10^{-11}
Neoprene rubber		3.988×10^{-10}	2.031×10^{-7}

The following graph illustrates how different materials affect the output voltage while maintaining a constant mode, shape, and size. As can be seen in Fig. 11, adding force leads to an increase in friction, which leads to an increase in output. However, after a short period of rotation, the material adjusts its alignment and loses some of the force applied. In addition to expedited material wear and unstable output voltage, this increase in output is accompanied by a more rapid rise in temperature, in addition to expedited material tear.

A fluorinated ethylene propylene (FEP) coupled with aluminum was used for the fixed part of this experiment, whereas Teflon, with a thickness of 1mm, was used for the rotational side, corresponding to the previous experiment. Additionally, a bridge diode was utilized to convert the output into direct current (DC), thereby extending the application potential.

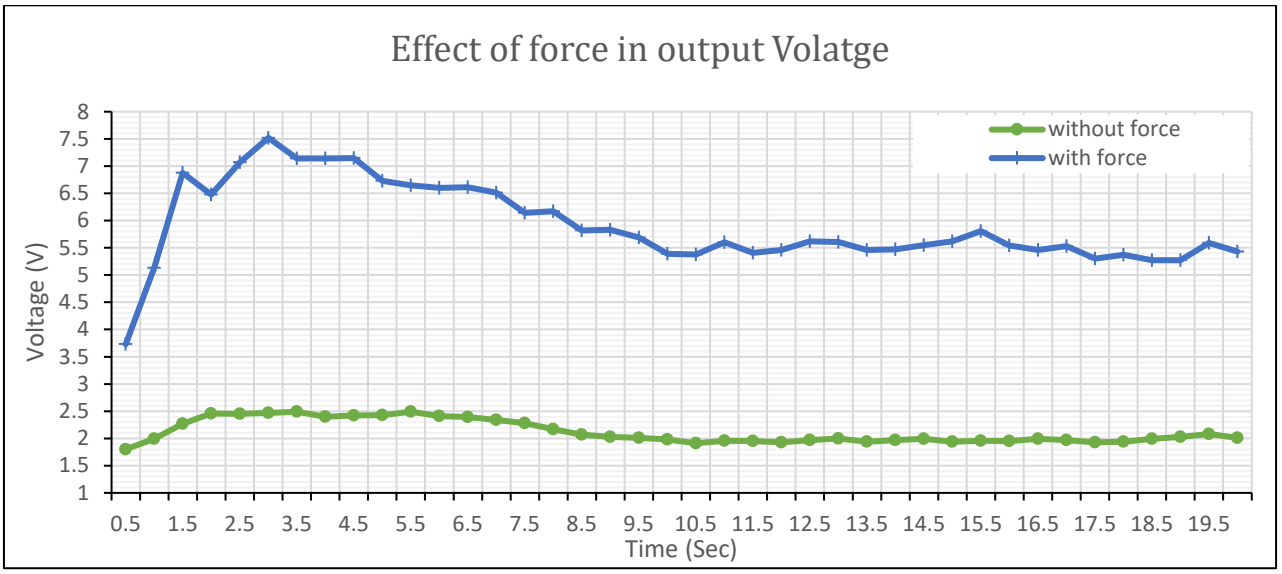

Fig. 9 *Graph showing the voltage response of TENG when adding force on the triboelectric layer*

A fascinating observation emerged when examining the effect of rotation speed on the output of the TENG. Increasing the rotation speed of the mini lathe machine has a similar effect compared to adding force on the triboelectric layer. This can be seen through the oscilloscope as shown in Fig. 12.

According to oscilloscope observations, the output signal frequency increases as the rotation speed is increased from 1500 to 2500 revolutions per minute (rpm). With this higher rotational frequency, the LED is illuminated continuously, which indicates a more consistent and smooth power output. Comparatively, as noted in the previous analysis, when force is applied to the system, the output voltage increases. Despite the similarity of this voltage boost and the increased rotation speed, the main difference lies in the waveform generated. Increased force enhances the output signal's amplitude, whereas increased rotation speed primarily influences its frequency and continuity as illustrated in Fig. 12.

Having these findings highlights the interaction between rotation speed, force, and the resulting output characteristics of TENG systems. Now, it is possible to tailor the TENG's performance to specific application requirements through the control and optimization of these parameters. Adjusting the rotation speed or adding force can be utilized strategically to achieve higher voltage outputs.

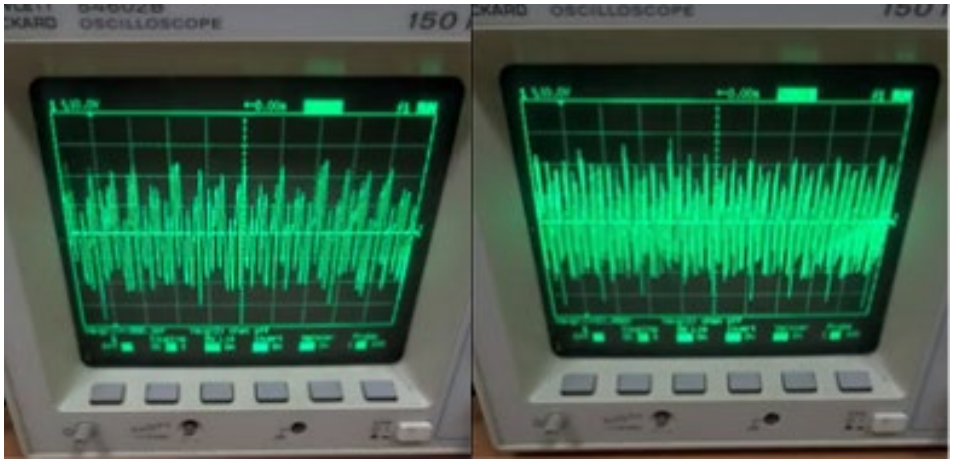

Fig. 10 *Waveforms depicting the impact of rotation speed on the intensity of the wave. The left side of the figure represents a rotation speed of 1500 (RPM), while the right side represents a rotation speed of 2500 RPM*

Freestanding triboelectric-layer mode performance in the TENG system is highly dependent on size and alignment. It is important to note that the layer size, including diameter and thickness, has a direct effect on the contact area and electrostatic charge generated. An increased contact area promotes a more effective interaction between triboelectric materials, resulting in improved performance and efficiency. In addition, the thickness of the layers influences the distance between the surfaces, resulting in a stronger triboelectric effect. To ensure efficient charge transfer while avoiding excessive separation that could cause decreased output, it is necessary to determine the optimal thickness.

To achieve success with freestanding triboelectric-layers, precise alignment is equally essential. Precise alignment ensures maximum contact between the layers, facilitating the transfer of charge and maximizing output voltage. Several factors contribute to misalignments, including reduced contact area, incomplete charge transfer, decreased performance, and uneven layer wear. The layers must be aligned accurately to ensure their centres are matched and their positions are evenly-spaced. Because force and rotational speed have a significant impact on the thickness of materials, maintaining consistent alignment during operation is challenging. In the freestanding triboelectric- layer mode of the TENG, attention to detail during assembly, the use of precise mounting fixtures, and efforts to minimize misalignment can increase output and efficiency significantly. Figure 13 shows a comparison between proper alignment against misalignment of materials during experiment.

Fig. 11 *A comparison between proper alignment on the left side and misalignment on the right side*

This study focuses on assessing the impact of different materials on the freestanding triboelectric- layer mode of the TENG. It relies heavily on average laboratory values and necessitated estimations for specific parameters due to equipment limitations. Factors such as capacitance changes in the rotating TENG, motor speed fluctuations, surface structure, electron affinity, and other material properties played a pivotal role in significantly influencing output voltage, power, and overall system performance.

6. Conclusion

This research has given researchers invaluable insights into optimizing power output and understanding its various factors that impact its performance by exploring a TENG with freestanding triboelectric-layer mode. Material selection plays a significant role in influencing the voltage output of TENGs; experiments using Teflon, silicone rubber, fiberglass, PVC and neoprene rubber among others had significant influences on its voltage output. Research has demonstrated that neoprene rubber produces the highest output voltage, showing how size and alignment play an essential role when operating the TENG. Diameter and thickness of layers have direct effects on contact area as well as charge transfer efficiency. Determining the appropriate thickness is vital to achieve balanced charge transfer and separation. When operating TENG's freestanding triboelectric-layer mode, alignment between layers must be optimized to maximize contact and facilitate full charge transfer. Consideration of these factors is vital in order to achieve maximum performance. As part of this research, the impact of rotation speed and force on output characteristics was studied, showing how they both influence voltage output while having different impacts on waveform characteristics. These findings contribute to a greater understanding and use of TENGs for harvesting clean energy from various mechanical resources, and it's anticipated that further research and development in this area will expand TENG technology's capabilities and practical applications.

Acknowledgement

FRGS, MOE and MMU support this research project with the Grant entitled: Formulating the Figure-of-Merits (FOM) for Optimizing the Output Power of Direct Current Triboelectric Nanogenerator (Project No: FRGS/1/2021/TK0/MMU/02/3). The research project is also devoted to those who have helped us.

Conflict of Interest

Authors declare that there is no conflict of interests regarding the publication of the paper.

Authors Contribution

The authors certify their contribution to the paper as follows: ***data gathering, analysis and presentation of results:*** *Khaled Jalal Mustafa Abd alnabi;* ***study conception, design and draft manuscript preparation:*** *Khaled Jalal Mustafa Abd alnabi and Lini Lee. The final version of the manuscript was reviewed and approved by all authors.*

References

[1] Wang, Z. L. (2013). Triboelectric Nanogenerators as New Energy Technology for Self-Powered Systems and as Active Mechanical and Chemical Sensors. ACS Nano, 7(11), 9533–9557. https://doi.org/10.1021/nn404614z

[2] Zhong Lin Wang, Long Lin, Jun Chen, Simiao Niu, Yunlong Zi. 2016. Green Energy and Technology Triboelectric Nanogenerator, *Springer*, 2-19. https://doi.org/10.3390/s23094195

[3] Zhang, H. (2019). Structures of Triboelectric Nanogenerators. In Flexible and Stretchable Triboelectric Nanogenerator Devices, Wiley online library, 19-40.

[4] Huang, Q.-A. (Ed.). (2018). Micro Electro Mechanical Systems. Micro/Nano Technologies, Springer,1335-1355.

[5] Zhou, Q., Pan, J., Deng, S., Xia, F., & Kim, T. (2021). Triboelectric Nanogenerator-Based Sensor Systems for Chemical or Biological Detection. Advanced Materials, Wiley online library, 2-21.

[6] Mengdi Han, Xiaosheng Zhang, Haixia Zhang. 2019. Flexible and Stretchable Triboelectric Nanogenerator Devices: Toward Self-powered Systems, *WILEY-VCH*, 19-24.

[7] Fan, F. R., Tian, Z. Q., & Wang, Z. L. (2012). Flexible triboelectric generator, Nano Energy, 1(2), 328-334. https://doi.org/10.1016/j.nanoen.2012.01.004.

[8] Zhu, G., Pan, C. F., Guo, W. X., Chen, C. Y., Zhou, Y. S., Yu, R. M., & Wang, Z. L. (2012), Triboelectric-generator-driven pulse electrodeposition for micropatterning, Nano Letters, 12(9), 4960-4965. https://doi.org/10.1021/nl302560k

[9] Wang, S. H., Lin, L., & Wang, Z. L. (2012). Nanoscale triboelectric-effect-enabled energy conversion for sustainably powering portable electronics, Nano Letters, 12(12), 6339-6346. https://doi.org/10.1021/nl303573d.

[10] Zhang, X. S., Han, M. D., Wang, R. X., Zhu, F. Y., Li, Z. H., Wang, W., & Zhang, H. X. (2013). Frequency-Multiplication High-Output Triboelectric Nanogenerator for Sustainably Powering Biomedical Microsystems, Nano Lett. 2013, 13(3), 1168–1172. https://doi.org/10.1021/nl3045684

[11] Wang, S. H., Lin, L., Xie, Y. N., Jing, Q. S., Niu, S. M., & Wang, Z. L. (2013). Sliding-Triboelectric Nanogenerators Based on in-Plane Charge-Separation Mechanism, Nano Lett. 2013, 13(5), 2226-2233. https://doi.org/10.1021/nl400738p

[12] Lin, L., Wang, S. H., Xie, Y. N., Jing, Q. S., Niu, S. M., Hu, Y. F., & Wang, Z. L. (2013). Segmentally structured disk triboelectric nanogenerator for harvesting rotational mechanical energy, Nano Letters, 13(6), 2916-2923. https//doi.org/ 10.1021/nl4013002

[13] Wang, S., Xie, Y., Niu, S., Lin, L., & Wang, Z. L. (2014). Freestanding Triboelectric-Layer-Based Nanogenerators for Harvesting Energy from a Moving Object or Human Motion in Contact and Non-contact Modes. Advanced Materials, 26(18), 2818–2824. https:/doi.org/10.1002/adma.201305303